



Wettability effects on mobilization of ganglia during displacement

Fanli Liu, Moran Wang*

Department of Engineering Mechanics, Tsinghua University, Beijing 100084, China

ARTICLE INFO

Keywords:

Multiphase flow
Wettability
Ganglia dynamics
Displacement
Porous media

ABSTRACT

Mobilization of trapped ganglia is of fundamental importance in two-phase displacement. Wettability alteration could be an effective approach to mobilizing ganglia, yet its feasibility as well as the impact of wettability in general lacks study. We investigate the wettability effects on trapped ganglia by theoretical analysis and numerical simulations for both fixed and altering wettability. For fixed wettability, it is found out that the critical pressure to mobilize trapped ganglia is symmetric about and usually peaks at the neutrally wet conditions (for simplicity, the invading and defending fluid are referred to as water and oil), but mobilized ganglia favor more water-wet conditions to be further displaced. This is due to the difference in the evolution of ganglia after initial mobilization under different wetting conditions: water-wetness contributes to the cooperative advancing of multiple interfaces, making ganglia continue moving as a whole, while oil-wetness leads to Haines jump in a single throat, which easily breaks up ganglia into smaller ones and leaves them trapped again. For altering wettability from oil-wet to water-wet through the transport of certain solute, we for the first time identify two crucial factors for the mobilization of ganglia. First, only the heterogeneous wetting state during the dynamic altering process enables the initial mobilization, whereas a step-wise alteration has little effect. Second, ganglia have to be able to merge with one another during the time window of the altering process for further displacement. Otherwise, an isolated trapped ganglion can only have limited mobilization at first by wettability alteration, and gets trapped again when the alteration is complete.

1. Introduction

Ganglia dynamics are important in two-phase flow, such as for CO₂ sequestration [1–3], soil renovation [4,5] and oil recovery [6–8]. For CO₂ sequestration the ganglia are expected to be stably trapped for geological time scale [9], while for oil recovery the goal is to recover the trapped oil ganglia, which often consists of more than 50% of oil in place in the reservoir after primary and secondary recovery processes [10,11]. Ganglia are trapped because the capillary drag force induced by their interfaces is strong enough to resist the viscous driving force induced by the external flow [8,12–14], and a well-known correlation of residual ganglia saturation against capillary number $Ca = \mu v / \sigma$ has been obtained by multiple experiments [14–19]. Here μ is the dynamic viscosity, v the external flow velocity and σ the interfacial tension, and Ca is proposed to describe the ratio of viscous force to capillary force. Experimental results showed that the residual ganglia saturation decreases logarithmically as Ca increases, agreeing with the physical picture that viscous force helps while capillary force impedes the mobilization of ganglia [14–19]. Consequently, two widely recognized

approaches to mobilizing ganglia are lowering the interfacial tension and increasing the inlet flow velocity [20–23]. The capillary number under reservoir conditions, however, can rarely be increased to the extent of mobilizing most ganglia [24,25].

On the other hand, wettability also has a considerable impact on the capillary force, which cannot be captured by the traditional definitions of capillary number. Wettability alteration induced by the transport of certain solute is one major mechanism of many enhanced oil recovery techniques, and it is also possible in nature [26–35]. It is likely that the solute-induced wettability alteration has the potential to mobilize trapped ganglia. Yet there has been a lack of studies on the wettability effects on the mobilization of ganglia. It has been identified in experiments that ganglia dynamics can be important in both water-wet [7,36] and non-water-wet conditions [37,38], but studies concerning the impact of wettability on two phase displacement have focused more on the pore-scale mechanisms that lead to trapping, such as snap-off and bypassing [39–43], or on obtaining the macroscopic correlations [44–49]. It is worth noting that even in those intensively studied aspects of wettability effects there are still debates and controversies, especially

* Corresponding author.

E-mail address: mrwang@tsinghua.edu.cn (M. Wang).

on the pore-scale impact of wettability [27,50–52], one important reason for which can be that the dynamic process of wettability alteration has not been considered in most works [27]. It is only in recent years that researchers have started to couple the dynamic wettability alteration process with two-phase displacement [53–55], but in terms of its impact on ganglia dynamics much remains unclear.

This paper studies the pore-scale ganglia dynamics under different wetting conditions and during wettability alteration. We first analyze and validate the conditions required to mobilize trapped ganglia and their further evolution after initial mobilization under different fixed wetting conditions, then we do similar investigations on the two-phase displacement processes coupled with dynamic wettability alteration induced by advection-diffusion of certain solute. For the simplicity of expression and without losing generality, in the following text the invading and defending fluid will be, respectively referred to as water and oil.

2. Numerical methods

The mobilization of trapped ganglia through solute-induced wettability alteration involves the two-phase fluid flow, and the advection-diffusion of certain solute. We solve the two-phase fluid flow with the color-gradient lattice Boltzmann method (LBM) [56–58] and solve the advection-diffusion equation (ADE) with the corresponding lattice Boltzmann method [59], both on a D2Q9 lattice. The details about each LBM are introduced in the supplementary material. The coupling of the two LBMs requires additional treatments. First, the solute should only be allowed in water and not in the oil phase. This is achieved by applying a recoloring step after collision in the LBM for ADE, which produces the following equation of state near the diffusive interface [59]:

$$\frac{C(x_w)}{C_{\max}} = x_w^\lambda, \quad (1)$$

where x is the percentage of water, $C(x_w)$ the corresponding concentration of solute at this position and C_{\max} the concentration at $x_w = 1$,

namely in the pure water phase. The exponent λ is an adjustable parameter controlling the extent of separation and is set to 1 in this work. The second treatment for coupling is that the wettability should be altered by the transport of solute. We adopt a non-linear relation between the contact angle θ of water and the concentration of solute locally, under the assumption of the Langmuir absorption model [53]:

$$\theta = (\theta_1 - \theta_0) \frac{(1 + K)C}{1 + K \bullet C} + \theta_0, \quad (2)$$

where θ_0 is the contact angle before alteration at $C = 0M$ and θ_1 is the contact angle after full alteration at $C = 1M$, the concentration at the inlet. The parameter K is set to equal 100 in this work. This non-linear relation has been found to be capable of capturing the wettability alteration near the contact line more correctly than the commonly adopted linear relation [53]. Validations of the numerical methods are provided in the supplementary material.

The common numerical settings throughout this work are illustrated in Fig. 1. Within the dashed lines is the solid structure, either extracted from images of sandstone or manually designated for different purposes. Between the dashed lines and the two ends are two buffer regions to eliminate the end effects. At the inlet and outlet, the Zou–He constant velocity boundary and constant pressure boundary are, respectively applied. If ADE is to be solved, then for the transport of solute the anti-bounce-back boundary is applied at the inlet to achieve constant concentration and the Neumann boundary is applied at the outlet to achieve zero concentration gradient. The upper and lower boundaries are solid walls, where the bounce-back boundary is applied to achieve the no-slip condition for fluid flow and impermeable wall for the solute. The walls of the solid structure are treated the same way. The size of the whole simulation domain is 600 times 1300 grids with grid width $\Delta x = 2.5 \times 10^{-6}m$ and the buffer region at the inlet and outlet, respectively have the width of 40 and 60 grids.

The initial two-phase distributions are either generated randomly given the initial oil saturation, or simply a single oil ganglion in water for different purposes. Then the inlet velocity is applied until the flow

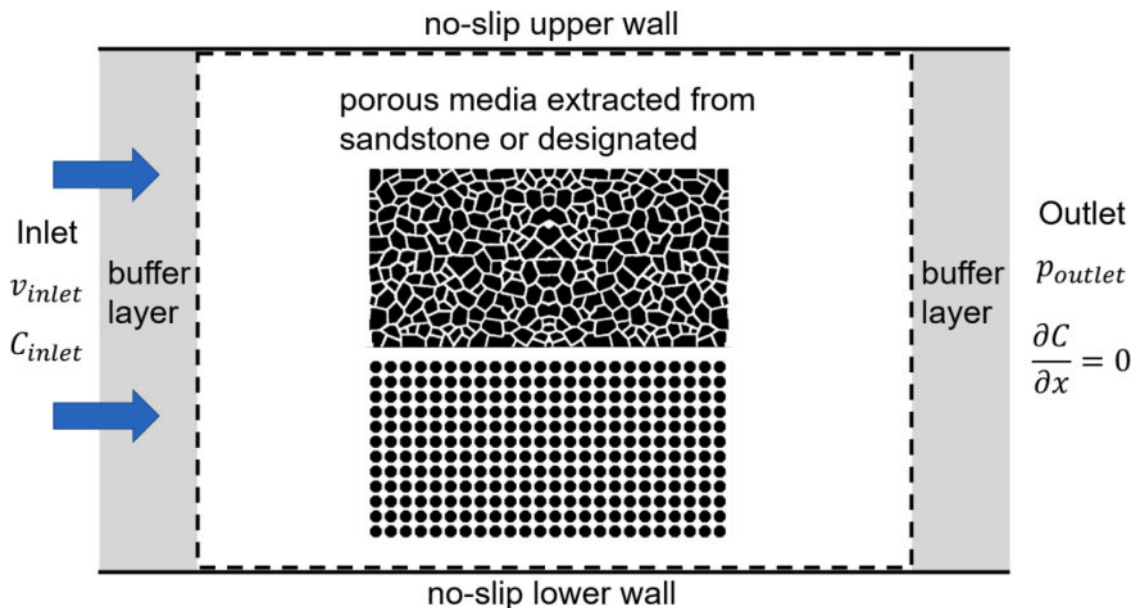


Fig. 1. The common numerical settings throughout this work. Within the dashed lines is the solid structure, either extracted from images of sandstone (the upper one) or manually designated for different purposes (the lower one). Between the dashed lines and the two ends are two buffer regions to eliminate the end effects. At the inlet and outlet, the Zou–He constant velocity boundary and constant pressure boundary are, respectively applied. If ADE is to be solved, then for the transport of solute the anti-bounce-back boundary is applied at the inlet to achieve constant concentration and the Neumann boundary is applied at the outlet to achieve zero concentration gradient. The upper and lower boundaries are solid walls, where the bounce-back boundary is applied to achieve the no-slip condition for fluid flow and impermeable wall for the solute. The walls of the solid structure are treated the same way. The size of the whole simulation domain is 600 times 1300 grids with grid width $\Delta x = 2.5 \times 10^{-6}m$ and the buffer region at the inlet and outlet, respectively have the width of 40 and 60 grids.

field is stable and all ganglia are trapped. This stabilized flow field is used as the initial condition for further simulation. In Sections 3.1 and 3.2, the wettability is fixed and the inlet velocity is increased gradually until the ganglia are mobilized. In Section 3.3, the inlet velocity is fixed and the concentration inlet is activated, allowing solute-induced wettability alteration.

Unless otherwise specified, the following physical parameters are adopted: density of water and oil $\rho_w = 1000\text{kg/m}^3$, $\rho_o = 1000\text{kg/m}^3$, viscosity of water and oil $\nu_w = 1 \times 10^{-6}\text{m}^2/\text{s}$, $\nu_o = 6 \times 10^{-6}\text{m}^2/\text{s}$, diffusion coefficient $D = 2.5 \times 10^{-8}\text{m}^2/\text{s}$ interfacial tension $\sigma = 0.01\text{N/m}$, inlet velocity $v_{inlet} = 2 \times 10^{-3}\text{m/s}$, inlet concentration $C_{inlet} = 1\text{M}$. The consequent capillary number is $Ca = \mu v/\sigma = 2 \times 10^{-4}$, which is much larger than that in the reservoir condition. We use this value because in numerical simulations an extremely small capillary number will either lead to instability or unbearably long computing time. This treatment will cause the discrepancy that in reservoir conditions much larger ganglia can still be trapped by capillary force, but will not affect our qualitative conclusions as the capillary force is strong enough to trap the ganglia in our simulations. In other words, the fact that all ganglia are trapped by the capillary force initially indicate that the displacement process is in the capillary-dominated regime. In addition, the diffusion coefficient here is one magnitude larger than that of common ions, but we have validated that a coefficient one magnitude smaller or larger than this value will produce similar qualitative results, shown in the supplementary materials.

3. Results and discussion

3.1. Impact of wettability on critical pressure for mobilization

A trapped ganglion will fail to maintain its stable state once the viscous pressure on it exceeds the resistant capillary pressure. But as the interfaces rearrange themselves locally, the capillary resistance can increase and the ganglion is again kept stationary unless the viscous pressure exceeds the largest local capillary resistance possible. Thus the value of this largest capillary resistance is the critical pressure for mobilization. Here we define any movement of the interface within the same pore or throat to be local rearrangement and not mobilization of the whole ganglion. The smaller the critical pressure, the easier ganglion can be mobilized.

We first give a theoretical analysis of the critical pressure to mobilize one ganglion. A ganglion can have many interfaces in the porous media, and the unbalance between viscous and capillary forces between any two interfaces will lead to mobilization. For simplicity, we only consider the two interfaces at the two ends in the direction of flow, because between these two interfaces the viscous pressure drop is the largest and statistically mobilization should mostly occur here. Then the critical pressure is essentially the sum of the capillary pressure at the two interfaces when they both yield the largest resistance. The capillary pressure P_c is given by:

$$P_c = \sigma \bullet \kappa, \quad (3)$$

where κ is the curvature of the interface and is dependent on the structure and contact angle. In the following analysis, we consider the two structures in Fig. 2(a), (b): a single channel and porous media. They both possess the significant converging-diverging feature that allows flexibility of the interfacial curvature. The single channel can be characterized by 3 parameters: the radius or half the width at the narrowest position, the ratio of the widest to the narrowest which we refer to as the aspect ratio A , and the diverging angle ϕ_1 , illustrated in Fig. 2(a), (b). The diverging angle is, viewed from the direction of the flow, how many degrees the walls expand compared with a parallel channel. It can be negative if the walls contract and not expand and a porous media must consist of both positive and negative diverging angles due to the converging-diverging feature. Assuming unit radius at the narrowest

position leaves two parameters A and ϕ_1 . Characterization of the porous media needs another parameter, the second diverging angle ϕ_2 due to throats at the sides, also shown in Fig. 2(a), (b). Within those structures, the capillary pressure of an interface can be expressed as

$$P_c = \sigma \cos(\theta_m + \varphi)/r, \quad (4)$$

where r and ϕ are the radius and the diverging angle that vary with position. Note that θ_m here is the contact angle of the invading phase as in Fig. 2(c), so at the front end which is closer to the inlet it is the contact angle of water but at the rear end it is the contact angle of oil. The extremes of capillary pressure must occur at either the narrowest or the widest positions, namely at $r = 1$ or $r = A$ while ϕ can still vary due to contact angle pinning at edges. For a single channel, after eliminating the unstable cases, the largest capillary resistance at the front interface depends on the contact angle as

$$\Delta P_1 = \begin{cases} \frac{\cos(\theta + \varphi_1)}{A}, \theta \in [0, \pi/2 - \varphi_1] \\ \cos(\min(\pi, \theta + \varphi_1)), \theta \in [\pi/2 - \varphi_1, \pi] \end{cases} \quad (5)$$

By Replacing θ with $\pi - \theta$ we obtain the largest resistance at the rear interface:

$$\Delta P_2 = \begin{cases} \cos(\min(\pi, \pi - \theta + \varphi_1)), \theta \in [0, \pi/2 + \varphi_1] \\ \frac{\cos(\pi - \theta + \varphi_1)}{A}, \theta \in (\pi/2 + \varphi_1, \pi] \end{cases} \quad (6)$$

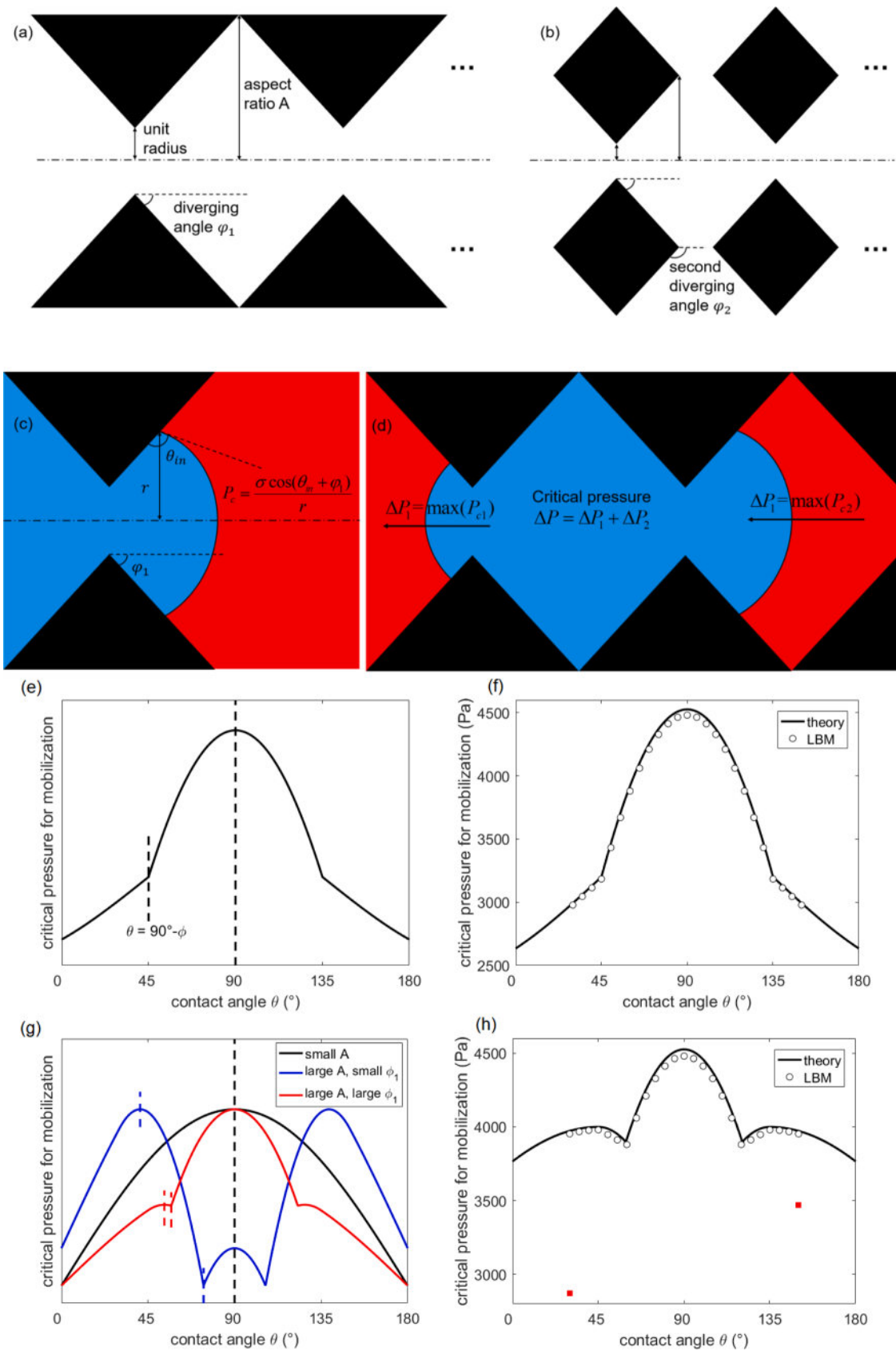
The critical pressure is then calculated as $\Delta P = \Delta P_1 + \Delta P_2$, illustrated in Fig. 2(d). Results are shown in Fig. 2(e). It is symmetric about $\theta=90^\circ$ and also peaks here. For porous media, where the largest capillary resistance of the front interface occurs depends additionally on the structural parameters. Similarly, the extremes must occur at either the narrowest or the widest position and two interfaces produce four possible cases. By comparing the capillary pressure for these four candidates at different structural parameters and contact angles, and after eliminating the unstable cases, the critical pressure in porous media can be classified in three qualitative types as shown in Fig. 2(g). The corresponding formulas are

$$\Delta P = \begin{cases} \frac{\cos(\min(\pi, \theta + \varphi_2))}{A} + \frac{\cos(\min(\pi, \pi - \theta + \varphi_2))}{A}, \text{small } A, \theta \in [0, \pi] \\ \frac{\cos(\min(\pi, \theta + \varphi_2))}{A} + \cos(\min(\pi, \pi - \theta + \varphi_1)), \text{large } A, \theta \in [0, \theta_c] \\ \cos(\min(\pi, \theta + \varphi_1)) + \cos(\min(\pi, \pi - \theta + \varphi_1)), \text{large } A, \theta \in [\theta_c, \pi - \theta_c] \\ \cos(\min(\pi, \theta + \varphi_1)) + \frac{\cos(\min(\pi, \pi - \theta + \varphi_2))}{A}, \text{large } A, \theta \in [\pi - \theta_c, \pi] \end{cases}, \quad (7)$$

$$\theta_c = \arctan\left(\frac{A \cos \varphi_1 - \cos \varphi_2}{A \sin \varphi_1 - \sin \varphi_2}\right).$$

In all cases the critical pressure is symmetric about $\theta=90^\circ$ as in the single channel, but it does not peak here if the aspect ratio A is large and at the same time the diverging angle ϕ_1 is small. For example, when $A = 3$ and $\varphi_1 < 38^\circ$. This alternate peak will be at $\theta = \arctan((A \sin \varphi_1 + \sin \varphi_2)/(A \cos \varphi_1 - \cos \varphi_2))$. However, large A and small ϕ_1 correspond to porous media consisting of very long and narrow channels, and are rare in real rocks. In addition, the curve with small A requires A to be closer to 1 and is also rare. It can be safely concluded that the critical pressure usually peaks at the neutral contact angle $\theta=90^\circ$.

We validate the theoretical analysis by LBM simulation. For a trapped ganglion, the flow velocity is gradually increased until the ganglion is mobilized, and the viscous pressure difference between the interfaces at the two ends is recorded as the critical pressure. In the previous analysis we treat the two interfaces independently, but they are actually under the restriction that the volume of the ganglion is constant.



(caption on next page)

Fig. 2. A series of figures concerning the investigation of the critical pressure. In (a) and (b) are the two structures considered for the investigation of the critical pressure in Section 3.1. They both have the crucial diverging-converging feature of general porous media. (a) A single diverging-converging channel. Unit radius is assumed at the narrowest throat, and this channel can be characterized by the diverging angle, defined as how many degrees the walls expand compared with a parallel channel viewed from the direction of the flow, and the aspect ratio, defined as the ratio of the radius at the widest pore to that at the narrowest throat. (b) A porous media consisting of diamond-shaped grains. Its characterization requires another parameter, the second diverging angle, which is defined similarly as the diverging angle, but at the widest instead of the narrowest position. (c) The capillary pressure in a diverging or converging channel can be derived as shown. The resulting expression can be understood as replacing the intrinsic contact angle with the effective contact angle. (d) The critical pressure of a ganglion is the sum of the capillary resistance at the front and rear interfaces. In (e) and (f) is the critical pressure for mobilization in the single channel as in Fig. 2(a). (e) The value obtained by theoretical analysis in Eqs. (5), (6). (f) Comparison between theory and LBM simulation. Both theory and simulation show that the critical pressure is symmetric about and peaks at the neutrally contact angle. In (g) and (h) is the critical pressure for mobilization in the porous media as in Fig. 2(b). (g) The value obtained by theoretical analysis in Eq. (7). (h) Comparison between theory and LBM simulation. Here we merely choose the most common case of large aspect ratio and large diverging angle for comparison. For most cases the critical pressure is still symmetric about and peaks at the neutral contact angle, with the exceptional case of large aspect ratio and small diverging angle where it peaks elsewhere. Large aspect ratio and small diverging angle correspond to porous media consisting of very long and narrow channels, and are rare in real rocks.

Therefore, in the simulation we adjust the volume of the ganglion to ensure that both interfaces can be at their maximum resistance, by setting the initial positions of the interfaces near the equilibrium positions derived. Since the qualitative trend of the critical pressure in porous media depends on the structural parameters, we choose the most common case of large A and large ϕ_1 to compare. Results are shown in Fig. 2(f) and (h) and they agree well with our analysis. The two deviating red points in Fig. 2(h) are due to that the ideal largest resistance cannot be reached because of the interference of other interfaces or walls.

These results indicate that the critical pressure is always symmetric about the neutral wettability, namely $\theta=90^\circ$, and usually peaks at $\theta=90^\circ$. More straightforwardly, the ganglia are hardest to be mobilized at $\theta=90^\circ$, and equally likely to be mobilized at water-wet and oil-wet conditions. This finding may be somewhat surprising as the more water-wet condition enhances the imbibition of water and thus should lower the critical pressure, but it can be intuitively understood by noting the fact that the mobilization of ganglia involves both water displacing oil at the front end and oil displacing water as the rear end. The capillary resistance provided by the front interface at, for example, $\theta=30^\circ$, equals the capillary resistance provided by the rear interface at $\theta=150^\circ$ because the invading phase at the rear end is oil and the contact angle of oil is also 30° , resulting in the symmetry of the critical pressure. The peak at the neutral contact angle is additionally related to the impact of the converging-diverging feature of the porous media. As Eq. (4) shows, the effective contact angle in calculating the capillary pressure is the intrinsic contact angle plus the diverging angle, meaning that an intrinsically neutral contact angle will lead to drainage. In water-wet or oil-wet conditions, imbibition at one end means drainage at another end. However, in neutrally wet condition, drainage occurs at both ends, and thus yields the highest capillary resistance in most cases.

3.2. Impact of wettability on evolvement of mobilized ganglia

In Section 3.1, we do theoretical analysis and numerical simulation on the critical pressure to mobilize the oil ganglia. Yet what we eventually care about is the displacement efficiency, defined as the percentage of ganglia displaced out, which also depends on the further evolvement after initial mobilization. In this section we carry out simulations with similar settings as that in Section 3.1: the inlet velocity is gradually increased from a small value to mobilize the ganglia. The difference is that this time the simulation goes on after ganglia are mobilized, and the velocity is further increased if all ganglia are trapped again. The initial phase distribution is generated as follows: we first divide the porous media evenly into small blocks having the size of a pore, and each block is randomly filled with water or oil depending on the given saturation. Then a test simulation starts until the phase distribution is stable. This stabilized distribution is adopted as the initial distribution for subsequent simulations. We have considered both the regular structure analyzed in Section 3.1 and the irregular sandstone-like structure shown in Fig. 1. For an initial oil saturation of 30% in the sandstone-like structure, the results of the displacement efficiency in

different wetting conditions in Fig. 3 show that the displacement efficiency increases monotonically as the system becomes more water-wet. This trend seems to be in contradiction with what the critical pressure implies, i.e. ganglia should be equally likely to be mobilized in water-wet and oil-wet conditions. We will show that the cause for this discrepancy is that the further evolvement of mobilized ganglia differs drastically in different wetting conditions.

Just before the ganglia are mobilized, interfaces should be at the state that yields the largest resistant capillary pressure. For strongly water-wet cases, the capillary pressure is a driving force at the front and Eq. (4) indicates that the interfaces tend to stay where both the radius and the diverging angle are the large, which is within a pore and at the junctions to other throats. As the interfaces approach this ideal state within a pore, they will merge and lose equilibrium in advance. This will lead to the cooperative advancing of interfaces, meaning flux comes from multiple channels and displaces the rest. In oil-wet cases, the interfaces tend to stay where the radius is small and the diverging angle is large, which is within a throat and at the throat-pore junction. No merging occurs as interfaces are at different junctions, and the interfaces often do not lose equilibrium simultaneously as the distance between different junctions leads to a non-negligible difference in viscous pressure. Therefore, when the interface at the front end loses equilibrium and the Haines jump occurs, it will be the only one here providing inward flux, and all other channels are being displaced. The displacing manner in the water-wet case tends to maintain the ganglia as a whole while that in the oil-wet case easily breaks up ganglia. When ganglia

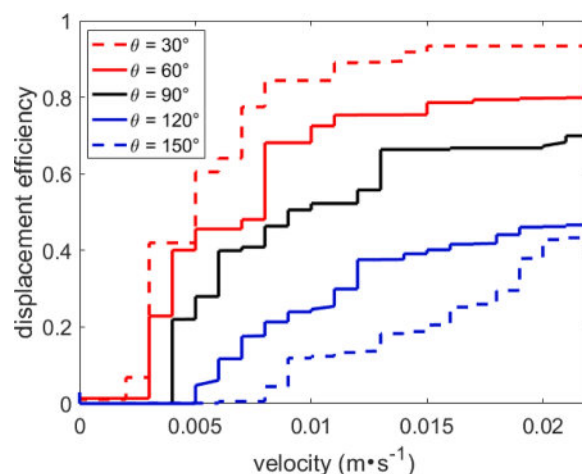


Fig. 3. The displacement efficiency for an initial oil saturation of 30% in the irregular sandstone-like structure, with gradually increasing velocity, under different wetting conditions. Results indicate a monotonically increasing displacement efficiency with increasing water-wetness, which is seemingly in contradiction with the previous finding that the ganglia are hardest to be mobilized at the neutral contact angle. It will be shown later that this is due to the different evolvements of ganglia in different wetting conditions.

break into smaller ones, the viscous pressure on them is decreased and they get trapped again. The difference between cooperative advancing in water-wet condition and the single channel Haines jump in the oil-wet condition is one major reason for the monotonic displacement efficiency against wettability we see in Fig. 3, and we observe this pore-scale difference by simulation, shown in Fig. 4(a).

There is another factor contributing to the monotonic trend against wettability. In porous media there are always spaces nearly perpendicular to the macroscopic flow direction, often being throats or part of throats. If an oil ganglion stably resides here, the viscous pressure on it will be extremely small and it is practically permanently trapped if one only intends to mobilize it through increasing flow velocity. Outside those spaces are usually diverging channels. In strongly water-wet condition, the advance of interface weakens the resistant capillary force and adds to further advancing, while in the oil-wet condition the advance of interface weakens the driving capillary force and impedes further advancing. Therefore, ganglia are more stable here if it is more oil-wet.

From the above analysis we can explain the typical evolutions of mobilized ganglia in water-wet and oil-wet conditions, as we also validate by numerical simulation in Fig. 4(b). In the water-wet condition, once the critical pressure is reached, interfaces at the front advance cooperatively and the ganglion continues advancing as a whole. While in oil-wet conditions, Haines jump occurs at one interface and this interface alone advances, pushing other interfaces back, leaving some trapped in throats at the sides and also decreasing the length of the main ganglion. The ganglion is then trapped again and a larger velocity is needed to remobilize it, until ganglia all reside within throats at the sides and being extremely hard to be mobilized by increasing velocity. We also note that breaking up of ganglia can happen in water-wet cases as well for large ganglia, but since they tend not to reside in throats, such breakups affect the length of ganglia little and they often continue advancing, shown in Fig. 4(c).

Additional simulations are performed in designated structures for the investigation of the influences of aspect ratio and coordination number and also for further validations. The structures are all similar to that in Fig. 2(b), with the aspect ratio modified by changing the shape of the solid and the coordination number modified by blocking some of the throats. Results of the final displacement efficiency are shown in Fig. 5. All cases show monotonically higher displacement efficiency in the more water-wet condition as in the previous result. The displacement efficiency is generally higher at smaller coordination number and larger

aspect ratio, especially in oil-wet cases, as small coordination number and large aspect ratio both decrease the volume of throats compared to pores, leaving less oil to be trapped and less reduction on the length of on the main ganglion in oil-wet condition, in agreement with our above conclusion.

Note that here snap-off does not occur since all the simulations are two-dimensional. Snap-off will break up ganglia into smaller ones in strongly water-wet conditions, but small ganglia also tend to merge into one again by the capillary waves generated during snap-off [60,61]. Thus we consider it still valid that the evolution of ganglia in water-wet conditions is better for the displacement of oil, though very strongly water-wet condition may be less favored than appropriately water-wet.

We further note that the consistency between the results obtained from the irregular sandstone-like structure and those from the designated regular structures is due to the inevitable converging-diverging feature of porous media. Although in Section 3.1 we only do theoretical derivations for the regular structures, the qualitative findings do not rely on the assumptions of the regularity. In any porous media there must be both diverging and converging channels, and generally all pore-throat junctions are either diverging or converging channels depending on the direction of the flow. There can be a few pore-throat junctions where the converging-diverging feature is not significant, but it can be safely assumed that there must be enough converging-diverging channels ubiquitous distributed throughout the porous media due to the random feature of the porous structure in nature. As interfaces advance, they must encounter those diverging channels every now and then and must overcome the extra capillary resistance to keep advancing, and that is all we need to do the theoretical analyses.

3.3. Mobilizing ganglia through wettability alteration

As we mentioned in the introduction, the approach of mobilizing ganglia by increasing flow velocity is limited, and in this section we aim to evaluate how ganglia can be mobilized through solute-induced wettability alteration. Similar to Sections 3.1 and 3.2, we consider both the critical pressure and the evolution after mobilization of oil ganglia. The critical pressure can be considerably lowered during wettability alteration when interfaces at the front are altered to water-wet while those at the rear remain oil-wet. This leads to imbibition at both ends, unlike in the homogeneous wetting condition where drainage must occur at one end. If a ganglion is mobilized by such reduction of

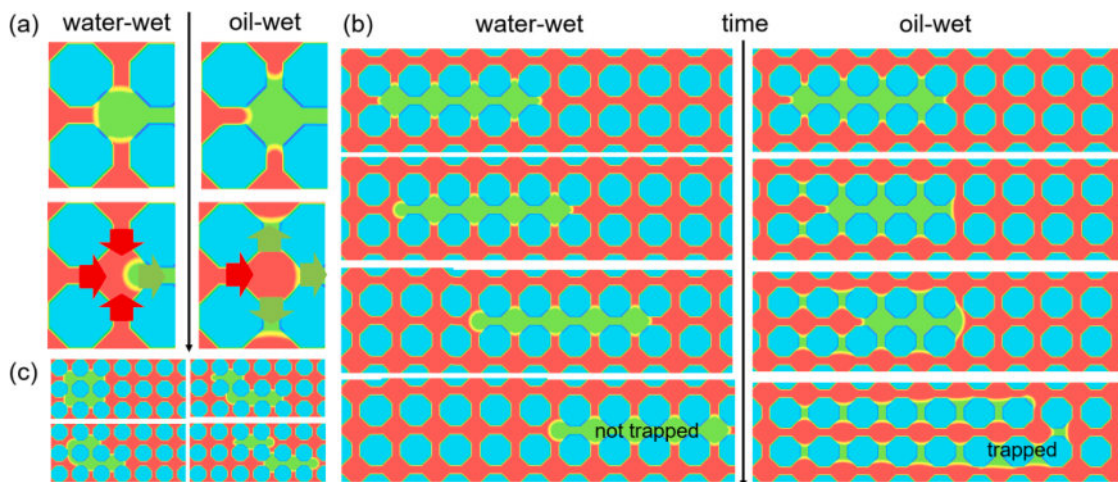


Fig. 4. Illustrations of the different evolutions of ganglia in different wetting conditions. (a) Cooperative advancing of multiple interfaces in water-wet conditions and Haines jump at a single interface in oil-wet condition, obtained by simulation. (b) The resulting different evolutions of a mobilized ganglion in different wetting conditions, obtained by simulation. In water-wet condition, cooperative advancing of front interfaces enables the ganglion to keep advancing as a whole, while in oil-wet condition, Haines jump tends to break ganglia into smaller ones, decrease the viscous pressure drop and impedes further advancement. (c) Large ganglion in water-wet may break up too, but often does not decrease the length of the ganglion and thus does not decrease the viscous pressure drop.

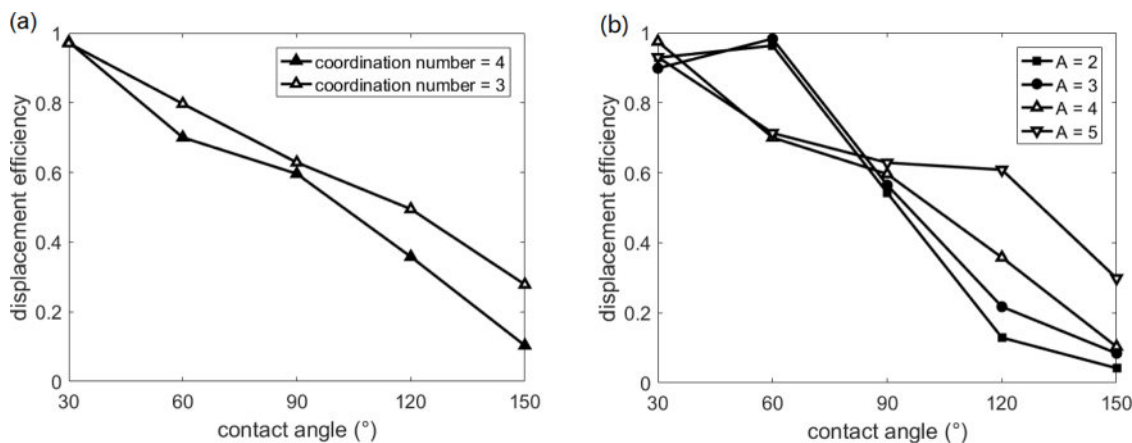


Fig. 5. (a) The displacement efficiency in different wetting conditions, for structures of different coordination numbers. (b) The displacement efficiency in different wetting conditions, for different aspect ratios. All cases show monotonically higher displacement efficiency in the more water-wet condition as in the previous result. The displacement efficiency is generally higher at smaller coordination number and larger aspect ratio, especially in oil-wet cases, as small coordination number and large aspect ratio both decrease the volume of throats compared to pores, leaving less oil to be trapped and less reduction on the length of on the main ganglion in oil-wet condition, in agreement with our above conclusion.

critical pressure, according to the conclusion in Section 3.2 the ganglion will tend to continue advancing since the front is altered to water-wet, as long as the critical pressure remains reduced by the heterogeneous wettability. The ganglion will get trapped again if wettability at the rear is also fully altered and it becomes homogeneous water-wet around the ganglion. That is, when the solute has transported to the rear end as well. Since the ganglion itself is also moving, there is a competition between the transport of solute and ganglion that determines the time window for the mobilization of the oil ganglion. Theoretically, we argue that since the movement of ganglia is actually flux in the whole channel, the solute will have as large the advection velocity of the ganglia. As the solute has an additional contribution of velocity by diffusion, the transport of solute must be faster than that of the ganglion and eventually it will reach the rear end. Therefore, we propose that for a single ganglion that does not interact with other ganglia, the range of its movement due to wettability alteration is always limited.

We perform simulations to validate the limited movement of the ganglion and also to show that this movement is usually too small to improve displacement efficiency by itself. The regular structure similar to that in Fig. 2(b) with $A = 4$, $\phi_1 = 45^\circ$ is adopted and we do non-dimensionalization by choosing the size of one pore to be the characteristic length. Initially one ganglion is trapped in the porous media in oil-wet condition, then solute begins to enter from the inlet. The initial length of oil ganglion, the degree of wettability alteration and the inlet velocity are varied to investigate their impact. Results are shown in Fig. 6. In all cases the ganglion gets trapped again after a finite movement that extends just several pores. A larger degree of wettability alteration and longer initial ganglion both increase this finite movement, as they both add to the difference between the viscous driving force and the capillary resistant force. The impact of velocity or capillary number is less clear as larger velocity increases the viscous force but also possibly shortens the time window for movement. Though the scale in our simulation is quite small, we argue that the results validate that a single ganglion can only have limited movement in two ways. First, in Fig. 6 we additionally simulate a special case where we manually give the system a step-wise change of wettability from oil-wet to water-wet, and in this case there is no movement of ganglion at all, which proves that the key to mobilization is the heterogeneous wetting condition induced by the dynamic transport of solute. Second, in the large scale the porous media itself is also much larger, and it will be more difficult for such finite movement to contribute to displacement.

The scenario is very different when ganglia can interact with each other, and the most important interaction here is the merge of two

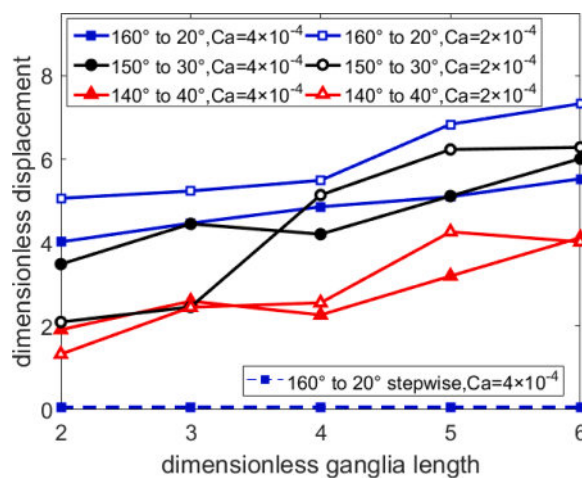


Fig. 6. The dimensionless displacement of non-interactive ganglia during displacement with solute-induced wettability alteration, at different ganglia lengths, degrees of wettability alteration and capillary numbers. The size of the periodic unit of the regular structure, which is also the size of one pore, is used as the characteristic length to do the non-dimensionalization. In all cases the ganglion gets trapped again after a finite movement that extends just several pores. A larger degree of wettability alteration and longer initial ganglion both increase this finite movement, as they both add to the difference between the viscous driving force and the capillary resistant force. The impact of velocity or capillary number is less clear as larger velocity increases the viscous force but also possibly shortens the time window for movement. A step-wise change of wettability from oil-wet to water-wet lead to no movement of ganglion at all, which proves that the key to mobilization is the heterogeneous wetting condition induced by the dynamic transport of solute.

ganglia when the rear ganglion is within the range of the limited movement of the front ganglion. This merge of ganglia has two major consequences. First, the range of the finite movement of the ganglion is extended because the length of the ganglion is increased. Second, ganglion grows larger by merging and once it becomes large enough, it will not be trapped again even after wettability at the rear end is altered. Since after full alteration the system becomes water-wet, according to Section 3.2 the ganglion will continue advancing and eventually contributes to displacement. The difference between the evolution of a single ganglion and multiple ganglia is illustrated in Fig. 7.

Therefore, the key to improving displacement efficiency through

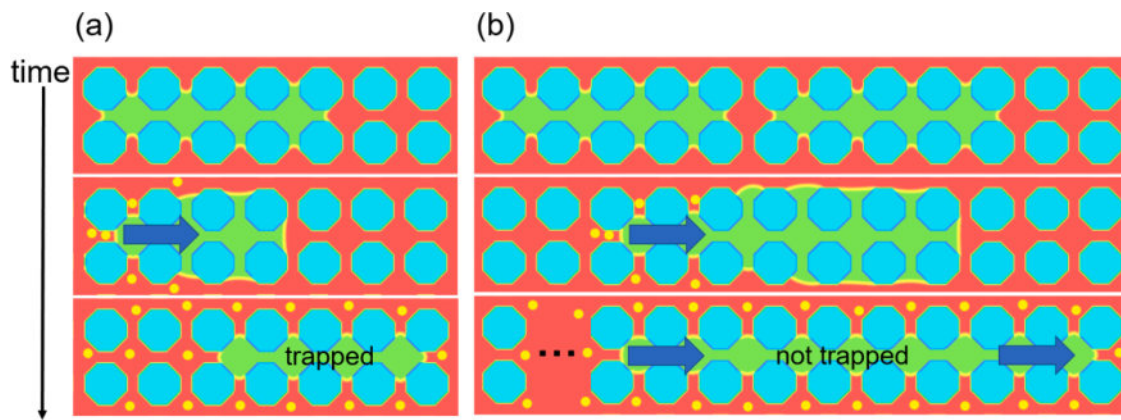


Fig. 7. (a) The evolution of a single ganglion under wettability alteration by simulation. The ganglion will have a limited movement due to the solute-induced heterogeneous wettability, and get trapped again after full alteration. (b) The evolution of a group of ganglia under wettability alteration by simulation. One mobilized ganglion can merge with another, extending the limited movement and growing larger. After full alteration, the ganglion can be large enough to not be trapped. The yellow dots stand for the solute that leads to wettability alteration. (For interpretation of the references to color in this figure legend, the reader is referred to the web version of this article.)

wettability alteration is the interaction between ganglia, caused by the limited movement during wettability alteration. Based on the above analysis we can make the following deductions about the displacement efficiency. The higher the initial saturation, the more interaction is possible and thus the higher efficiency. In addition, any factor that increases the range of movement should increase the probability of interaction thus also leads to higher efficiency. Simulations are performed in the irregular sandstone-like structure with varying initial oil saturation, flow velocity and degree of wettability alteration. The initial phase distribution is generated the same way as in Section 3.2. Results in Fig. 8 shows that the efficiency decreases with the decrease of initial oil saturation, especially at low saturation. The impact of flow velocity and degree of wettability alteration is consistent with their impact on the range of movement of a single ganglion in Fig. 6, in that larger movement corresponds to higher efficiency. A step-wise wettability alteration results in no displacement of oil at all, since it does not mobilize ganglia in the first place. These results all agree with our predictions and further validate our theory.

It is worth noting that all simulations in this work are performed in two-dimensional structure. It can directly correspond to the three-dimensional cases where the layer flow is not important, for example when the structure is not highly irregular. Since our work focuses on

mechanisms, excluding the layer flow can be one merit, as in three-dimensional experimental works the other mechanisms are mixed together with the impact of layer flow [62,63] and are more difficult to study.

4. Conclusion

This work investigates how wettability impacts the mobilization of trapped ganglia and the approach of mobilizing ganglia through wettability alteration, with the help of theoretical and numerical tools.

For fixed wettability, it is found out that ganglia are usually hardest to be mobilized in the neutrally wet condition and equally likely to be mobilized in water-wet and oil-wet condition. However, mobilized ganglia favor more water-wet condition because the subsequent evolution after initial mobilization distinctively differs in different wetting conditions, resulting in a monotonically increasing displacement efficiency with increased water-wetness.

For solute-induced altering wettability, two crucial factors are identified for the mobilization of ganglia: the heterogeneous wetting state caused by the dynamic altering process and the merge of ganglia. The solute-induced heterogeneous wetting state enables imbibition at both ends of the ganglia and considerably decreases the critical pressure.

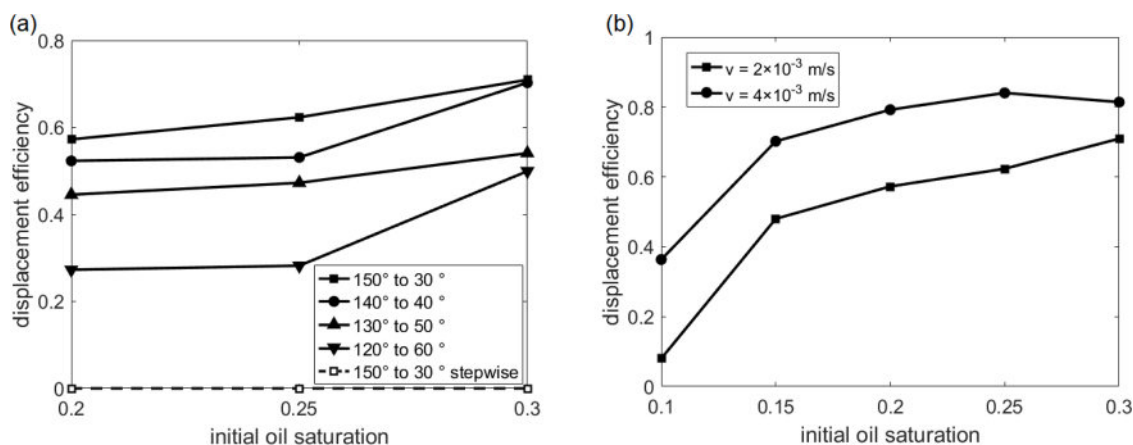


Fig. 8. The displacement efficiency in the irregular sandstone-like structure by displacement with solute induced wettability alteration, with varying initial oil saturation, degree of alteration and inlet flow velocity. The efficiency decreases with the decrease of initial oil saturation, especially at low saturation, because the merge of ganglia is less likely. The impact of flow velocity and degree of wettability alteration is consistent with their impact on the range of movement of a single ganglion in Fig. 6, in that larger movement corresponds to higher efficiency. A step-wise wettability alteration results in no displacement of oil at all, since it does not mobilize ganglia in the first place.

However, after full alteration the ganglia will be trapped again, unless merge of ganglia makes the ganglia large enough to overcome the capillary resistance.

To the authors' knowledge, this is the first work to investigate such wettability effects on the mobilization of trapped ganglia, in comparison to the previous works that focus on the impact of interfacial tension or velocity [18,20]. This work helps deepen the understanding of the impact of wettability on two phase displacement.

CRedit authorship contribution statement

Fanli Liu: Investigation, Software, Validation, Writing – original draft. **Moran Wang:** Conceptualization, Supervision, Writing – review & editing, Project administration.

Declaration of Competing Interest

The authors declare that they have no known competing financial interests or personal relationships that could have appeared to influence the work reported in this paper.

Acknowledgments

The authors thank the National Key R&D Program of China (No. 2019YFA0708704), NSF grant of China (No. U1837602) and the Tsinghua University Initiative Scientific Research Program for financial support.

Supplementary materials

Supplementary material associated with this article can be found, in the online version, at doi:10.1016/j.ijmecs.2021.106933.

Reference

- Pentland C, El-Maghraby R, Georgiadis A, Iglauer S, Blunt M. Immiscible displacements and capillary trapping in CO₂ storage. *Energy Procedia* 2011;4: 4969–76.
- Krevor SC, Pini R, Li B, Benson SM. Capillary heterogeneity trapping of CO₂ in a sandstone rock at reservoir conditions. *Geophys Res Lett* 2011;38(15).
- Ide ST, Jessen K, Orr FM. Storage of CO₂ in saline aquifers: effects of gravity, viscous, and capillary forces on amount and timing of trapping. *Int J Greenh Gas Control* 2007;1(4):481–91.
- Qian T, Huo L, Zhao D. Laboratory investigation into factors affecting performance of capillary barrier system in unsaturated soil. *Water Air Soil Pollut* 2010;206(1): 295–306.
- McCartney JS, Zornberg JG. Effects of infiltration and evaporation on geosynthetic capillary barrier performance. *Can Geotech J*. 2010;47(11):1201–13.
- Armstrong RT, McClure JE, Berrill MA, Rucker M, Schlüter S, Berg S. Beyond Darcy's law: the role of phase topology and ganglion dynamics for two-fluid flow. *Phys Rev E* 2016;94(4):043113.
- Rucker M, Berg S, Armstrong R, Georgiadis A, Ott H, Schwing A, et al. From connected pathway flow to ganglion dynamics. *Geophys Res Lett* 2015;42(10): 3888–94.
- Payatakes A. Dynamics of oil ganglia during immiscible displacement in water-wet porous media. *Annu Rev Fluid Mech* 1982;14(1):365–93.
- Ren B, Sun Y, Bryant S. Maximizing local capillary trapping during CO₂ injection. *Energy Procedia* 2014;63:5562–76.
- Thomas S. Enhanced oil recovery—an overview. *Oil Gas Sci Technol Rev IFP* 2008; 63(1):9–19.
- Tunio SQ, Tunio AH, Ghirano NA, El Adawy ZM. Comparison of different enhanced oil recovery techniques for better oil productivity. *Int J Appl Sci Technol* 2011;1 (5).
- Larson R, Scriven L, Davis H. Percolation theory of residual phases in porous media. *Nature* 1977;268(5619):409–13.
- Melrose J. Role of capillary forces in determining microscopic displacement efficiency for oil recovery by waterflooding. *J Can Pet Technol* 1974;13(04).
- Ng K, Davis H, Scriven L. Visualization of blob mechanics in flow through porous media. *Chem Eng Sci* 1978;33(8):1009–17.
- Geistlinger H, Ataei-Dadavi I, Mohammadian S, Vogel HJ. The impact of pore structure and surface roughness on capillary trapping for 2D and 3D porous media: comparison with percolation theory. *Water Resour Res* 2015;51(11):9094–111.
- Morrow N, Songkran B. Effect of viscous and buoyancy forces on nonwetting phase trapping in porous media. *Surface phenomena in enhanced oil recovery*. Springer; 1981. p. 387–411.
- Suekane T, Zhou N, Hosokawa T, Matsumoto T. Direct observation of trapped gas bubbles by capillarity in sandy porous media. *Transp Porous Media* 2010;82(1): 11–22.
- Wildenschild D, Armstrong RT, Herring AL, Young IM, Carey JW. Exploring capillary trapping efficiency as a function of interfacial tension, viscosity, and flow rate. *Energy Procedia* 2011;4:4945–52.
- Guo H, Dou M, Hanqing W, Wang F, Yuanqun G, Yu Z, et al. Proper use of capillary number in chemical flooding. *J Chem* 2017;2017.
- Jamaloei BY, Kharrat R. Fundamental study of pore morphology effect in low tension polymer flooding or polymer-assisted dilute surfactant flooding. *Transp Porous Media* 2009;76(2):199–218.
- Larson R. Analysis of the physical mechanisms in surfactant flooding. *Soc Pet Eng J* 1978;18(01):42–58.
- Foster W. A low-tension waterflooding process. *J Pet Technol* 1973;25(02):205–10.
- Mai A, Kantzas A. Heavy oil waterflooding: effects of flow rate and oil viscosity. *J Can Pet Technol* 2009;48(03):42–51.
- Guo H, Dou M, Hanqing W, Wang F, Yuanqun G, Yu Z, et al. Review of capillary number in chemical enhanced oil recovery. In: *Proceedings of the SPE Kuwait oil and gas show and conference*. OnePetro; 2015.
- Guo H, Song K, Hilfer R. A critical review of capillary number and its application in enhanced oil recovery. In: *Proceedings of the SPE improved oil recovery conference*. OnePetro; 2020.
- Bartels WB, Mahani H, Berg S, Hassanzadeh S. Literature review of low salinity waterflooding from a length and time scale perspective. *Fuel* 2019;236:338–53.
- Liu F, Wang M. Review of low salinity waterflooding mechanisms: wettability alteration and its impact on oil recovery. *Fuel* 2020;267:117112.
- Liu F, Wang M. Electrokinetic mechanisms and synergistic effect on ion-tuned wettability in oil-brine-rock systems. *Transp Porous Media* 2021:1–20.
- Sheng JJ. Critical review of low-salinity waterflooding. *J Pet Sci Eng* 2014;120: 216–24.
- Ahmadi MA, Galedarzadeh M, Shadizadeh SR. Wettability alteration in carbonate rocks by implementing new derived natural surfactant: enhanced oil recovery applications. *Transp Porous Media* 2015;106(3):645–67.
- Delshad M, Najafabadi NF, Anderson G, Pope GA, Sepehrnoori K. Modeling wettability alteration by surfactants in naturally fractured reservoirs. *SPE Reserv Eval Eng* 2009;12(03):361–70.
- Gong H, Li Y, Dong M, Ma S, Liu W. Effect of wettability alteration on enhanced heavy oil recovery by alkaline flooding. *Colloids Surf A Physicochem Eng Asp* 2016;488:28–35.
- Seethepalli A, Adibhatla B, Mohanty K. Wettability alteration during surfactant flooding of carbonate reservoirs. In: *Proceedings of the SPE/DOE symposium on improved oil recovery*. OnePetro; 2004.
- Mohammed M, Babadagli T. Wettability alteration: a comprehensive review of materials/methods and testing the selected ones on heavy-oil containing oil-wet systems. *Adv Colloid Interface Sci* 2015;220:54–77.
- Misyura S. Dependence of wettability of microtextured wall on the heat and mass transfer: simple estimates for convection and heat transfer. *Int J Mech Sci* 2020; 170:105353.
- Avraam D, Payatakes A. Flow regimes and relative permeabilities during steady-state two-phase flow in porous media. *J Fluid Mech* 1995;293:207–36.
- Lin Q, Bijeljic B, Berg S, Pini R, Blunt MJ, Krevor S. Minimal surfaces in porous media: pore-scale imaging of multiphase flow in an altered-wettability bentheimer sandstone. *Phys Rev E* 2019;99(6):063105.
- Zou S, Armstrong RT, Arns JY, Arns CH, Hussain F. Experimental and theoretical evidence for increased ganglion dynamics during fractional flow in mixed-wet porous media. *Water Resour Res* 2018;54(5):3277–89.
- Alyafei N, Blunt MJ. The effect of wettability on capillary trapping in carbonates. *Adv Water Resour* 2016;90:36–50.
- Mohammadmoradi P, Kantzas A. Pore scale investigation of wettability effect on waterflood performance. In: *Proceedings of the SPE annual technical conference and exhibition*. OnePetro; 2016.
- Mohanty KK, Davis HT, Scriven L. Physics of oil entrapment in water-wet rock. *SPE Reserv Eng* 1987;2(01):113–28.
- Suicmez VS, Piri M, Blunt MJ. Effects of wettability and pore-level displacement on hydrocarbon trapping. *Adv Water Resour* 2008;31(3):503–12.
- Yu L, Wardlaw NC. The influence of wettability and critical pore-throat size ratio on snap-off. *J Colloid Interface Sci* 1986;109(2):461–72.
- Akai T, Alhammadi AM, Blunt MJ, Bijeljic B. Modeling oil recovery in mixed-wet rocks: pore-scale comparison between experiment and simulation. *Transp Porous Media* 2019;127(2):393–414.
- Gharbi O, Blunt MJ. The impact of wettability and connectivity on relative permeability in carbonates: a pore network modeling analysis. *Water Resour Res* 2012;48(12).
- Kallel W, Van Dijke MJ, Sorbie KS, Wood R, Jiang Z, Harland S. Modeling the effect of wettability distributions on oil recovery from microporous carbonate reservoirs. *Adv Water Resour* 2016;95:317–28.
- Zhao J, Kang Q, Yao J, Viswanathan H, Pawar R, Zhang L, et al. The effect of wettability heterogeneity on relative permeability of two-phase flow in porous media: a lattice Boltzmann study. *Water Resour Res* 2018;54(2):1295–311.
- Zhao X, Blunt MJ, Yao J. Pore-scale modeling: effects of wettability on waterflood oil recovery. *J Pet Sci Eng* 2010;71(3–4):169–78.
- Luo J, Wu SY, Xiao L, Chen ZL. Parametric influencing mechanism and control of contact time for droplets impacting on the solid surfaces. *Int J Mech Sci* 2021;197: 106333.
- Jadhunandan P, Morrow NR. Effect of wettability on waterflood recovery for crude-oil/brine/rock systems. *SPE Reserv Eng* 1995;10(01):40–6.

- [51] Morrow N, Buckley J. Improved oil recovery by low-salinity waterflooding. *J Pet Technol* 2011;63(05):106–12.
- [52] AlRatrou A, Blunt MJ, Bijeljic B. Wettability in complex porous materials, the mixed-wet state, and its relationship to surface roughness. *Proc Natl Acad Sci* 2018; 115(36):8901–6.
- [53] Akai T, Blunt MJ, Bijeljic B. Pore-scale numerical simulation of low salinity water flooding using the lattice Boltzmann method. *J Colloid Interface Sci* 2020;566: 444–53.
- [54] Aziz R, Joekar-Niasar V, Martínez-Ferrer PJ, Godinez-Brizuela OE, Theodoropoulos C, Mahani H. Novel insights into pore-scale dynamics of wettability alteration during low salinity waterflooding. *Sci Rep* 2019;9(1):1–13.
- [55] Aziz R, Niasar V, Erfani H, Martínez-Ferrer PJ. Impact of pore morphology on two-phase flow dynamics under wettability alteration. *Fuel* 2020;268:117315.
- [56] Leclaire S, Reggio M, Trépanier JY. Numerical evaluation of two recoloring operators for an immiscible two-phase flow lattice Boltzmann model. *Appl Math Model* 2012;36(5):2237–52.
- [57] Leclaire S, El-Hachem M, Trépanier JY, Reggio M. High order spatial generalization of 2D and 3D isotropic discrete gradient operators with fast evaluation on GPUs. *J Sci Comput* 2014;59(3):545–73.
- [58] Akai T, Bijeljic B, Blunt MJ. Wetting boundary condition for the color-gradient lattice Boltzmann method: validation with analytical and experimental data. *Adv Water Resour* 2018;116:56–66.
- [59] Riaud A, Zhao S, Wang K, Cheng Y, Luo G. Lattice-Boltzmann method for the simulation of multiphase mass transfer and reaction of dilute species. *Phys Rev E* 2014;89(5):053308.
- [60] Rücker M, Berg S, Armstrong R, Georgiadis A, Ott H, Simon L, et al. The fate of oil clusters during fractional flow: trajectories in the saturation-capillary number space. In: *Proceedings of the conference international symposium of the society of core analysts*. 7; 2015. 2015.
- [61] Liu Z, Herring A, Arns C, Berg S, Armstrong RT. Pore-scale characterization of two-phase flow using integral geometry. *Transp Porous Media* 2017;118(1):99–117.
- [62] Dandapat B, Singh S, Maity S. Thin film flow of bi-viscosity liquid over an unsteady stretching sheet: an analytical solution. *Int J Mech Sci* 2017;130:367–74.
- [63] Liu X, Zhang H, Wang F, Xia G, Li Z, Zhu C, et al. Numerical investigation of flow behavior and film thickness in the single screw expander. *Int J Mech Sci* 2021;190: 106047.